PROPERTIES OF EXCITON AND EXCITON-POLARON: EXACT NUMERIC SOLUTION.

A.S. Mishchenko[1,2], N. Nagaosa[1,3], N.V. Prokof'ev[4], B.V. Svistunov[2], and E.A. Burovski[2]

(1) Correlated Electron Research Center, AIST, Tsukuba Central 4, Tsukuba 305-8562, Japan
(2) RRC 'Kurchatov Institute', 123182, Moscow, Russia
(3) Department of Applied Physics, The University of Tokyo, 7-3-1 Hongo, Bunkyo-ku, Tokyo 113, Japan
(4) Department of Physics, University of Massachusetts, Amherst, Massachusetts 01003

We developed a Monte Carlo method of calculation of Green function in imaginary times which is free from systematic errors for the case of quasiparticle in a boson bath [1,2]. A novel procedure of analytic continuation [1], which is free from systematic errors, provides a tool for study of optical spectra of quasiparticles. Our method does not rely on the specific form of the quasiparticle dispersion and properties of boson bath.

As a specific examples we consider Frohlich [1] and Holstein polaron. Calculating within free from approximation approach the current-current correlation function and making the numeric analytic continuation we obtain exact data for the optic response of polarons.

We generalize the method to get a precise numeric solution of the irreducible two-body problem and apply it to excitons in solids [3,4]. Our method does not rely on the specific form of the electron and hole dispersion laws and is valid for any attractive electron-hole potential. We establish limits of validity of the Wannier (large radius) and Frenkel (small radius) approximations, present accurate data for the intermediate radius excitons, and give evidence for the charge transfer nature of the monopolar exciton in mixed valence materials.

Finally, we discuss generalization of the method to the case of exciton in phonon field and extend the technique for the t-J model [5] to the case of interaction of the hole with optical phonons.

REFERENCES:

1. A.S Mishchenko, N.V.Prokof'ev, A.Sakamoto, and B.V.Svistunov, Phys. Rev. B, vol. 62, 6317 (2000)
2. A.S Mishchenko and N. Nagaosa, Phys. Rev. Lett., vol. 86, 4624 (2001)
3. E.A. Burovski, A.S. Mishchenko, N.V.Prokof'ev, and B.V.Svistunov, Phys. Rev. Lett., vol. 87, 6402 (2001)
4. A.S Mishchenko, N. Nagaosa, N.V.Prokof'ev, A.Sakamoto, and B.V.Svistunov, Phys. Rev. B, vol. 66, 020301(R) (2002).
5. A.S Mishchenko, N.V.Prokof'ev, and B.V.Svistunov, Phys. Rev. B, vol. 64, 033101 (2001).

- **Description of the techniques of exact generation of Matsubara Green function of the quasiparticles in bosonic bath.**
- **Description of the exact method of analytic continuation to the real energies.**
- **Generalization of the technique to two-particle Green function: exciton.**
- **Several application of the technique: Rashba-Pekar exciton, charge-transfer exciton.**
- **Magical number '4' for Fröhlich polaron. Lehman function and optical response.**
- **Further generalization: quasiparticle in two bosonic bathes. t-J model in phonon field.**

Quasiparticle in the boson bath: Fröhlich polaron and Rashba-Pekar exciton

$$H = H_e + H_{ph} + H_{e\text{-}ph} \,.$$

Quasiparticle dispersion:

$$H_e = \sum_{\mathbf{k}} \varepsilon(\mathbf{k})\, a_{\mathbf{k}}^\dagger a_{\mathbf{k}} \,.$$

Boson dispersion:

$$H_{ph} = \sum_{\mathbf{q}} \omega_{\mathbf{q}}\, b_{\mathbf{q}}^\dagger b_{\mathbf{q}} \,.$$

Quasiparticle-boson interaction:

$$H_{e\text{-}ph} = \sum_{\mathbf{k},\mathbf{q}} V(\mathbf{q}) \left(b_{\mathbf{q}}^\dagger - b_{-\mathbf{q}} \right) a_{\mathbf{k}-\mathbf{q}}^\dagger a_{\mathbf{k}} \,.$$

Although presented technique is suitable for arbitrary dispersion of quasi-particle, arbitrary dispersion of phonons and valid for arbitrary vortex of quasiparticle-boson interaction, I'll show the results for the continuous model

$$\varepsilon(\mathbf{k}) = k^2/2; \quad \omega_{\mathbf{q}} = 1.$$

in two specific cases.

I. Fröhlich polaron (long-range interaction):

$$V_{FR}(\mathbf{q}) = i \left(2\sqrt{2}\alpha\pi \right)^{1/2} \frac{1}{q} \,.$$

II. Exciton-polaron (short-range interaction):

$$V_{EX}(\mathbf{q}) = V_{FR}(\mathbf{q}) \left\{ \frac{1}{[1+(p_e a_B q/2)^2]^2} - \frac{1}{[1+(p_h a_B q/2)^2]^2} \right\}.$$

Here $p_{e,h} = m_{e,h}/(m_e + m_h)$ and a_B is the Bohr radius.

Diagrammatic Feinman expansion for Matsubara Green function

Expansion can be transformed into a series of **positively definite** integrals with ever increasing number of integration variables.

$$G(\mathbf{k},\tau) = \sum_{n=0,2,4,\ldots}^{\infty} \int_{\tau}^{0} d\tau_n \int_{\tau_n}^{0} d\tau_{n-1} \ldots \int_{\tau_2}^{0} d\tau_1 \times$$

$$\int d\mathbf{q}_1 \int d\mathbf{q}_2 \ldots \int d\mathbf{q}_{n/2} \mid V(\mathbf{q}_1) \mid^2 \mid V(\mathbf{q}_2) \mid^2 \ldots \mid V(\mathbf{q}_{n/2}) \mid^2 \times$$

$$G^{(0)}(\mathbf{k}, \tau_1 - 0) G^{(0)}(\mathbf{k}-\mathbf{q}_1, \tau_2 - \tau_1) \ldots G^{(0)}(\mathbf{k}, \tau - \tau_{n-1})$$

$$D(\mathbf{q}_1, \tau' - \tau_1) \ldots D(\mathbf{q}_1, \tau_n - \tau'')$$

Here

$$G^{(0)}(\mathbf{k},\tau) = \exp\{-(\varepsilon(\mathbf{k}) - \mu)\tau\}; \; D(\mathbf{q},\tau) = \exp\{-\omega_{\mathbf{q}}\tau\}$$

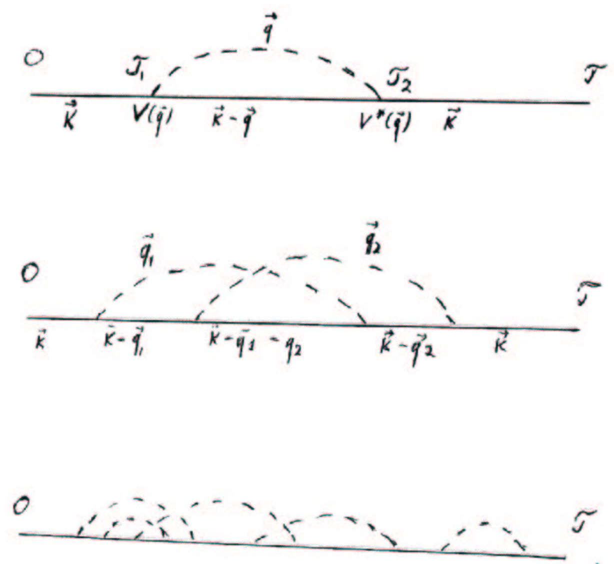

How to extract an information

$$G(\vec{k},\tau)=\sum_{\nu} |\langle \nu | a_k^{+} | VAC\rangle|^2 e^{-[E_\nu(\vec{k})-E_{VAC}]\tau}$$

$$\boxed{\begin{gathered} G(\vec{k},\tau)=\int_0^\infty d\omega\, g_k(\omega) e^{-\omega\tau} \\ g_k(\omega)=\sum_{\nu} |\langle \nu | a_k^{+} | VAC\rangle|^2 \delta[\omega-\varepsilon_\nu(k)] \end{gathered}}$$

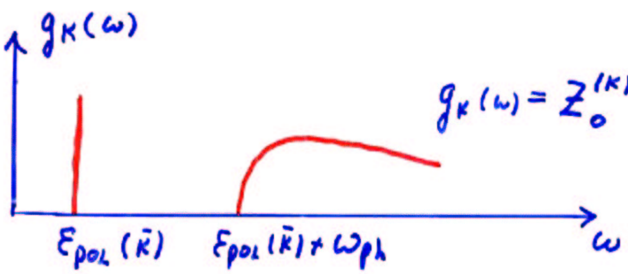

$$g_k(\omega)=Z_0^{(k)}\delta[\omega-\varepsilon_{pol}(k)]+\dots$$

$$G(\vec{k},\tau >> \omega_{ph}^{-1}) \rightarrow Z_0^{(\vec{k})} e^{-\varepsilon_{pol}(\vec{k})\tau}$$

$$\boxed{\ln G(\vec{k},\tau >> \omega_{ph}^{-1}) \rightarrow \ln Z_0^{(\vec{k})} - \varepsilon_{pol}(\vec{k})\tau}$$

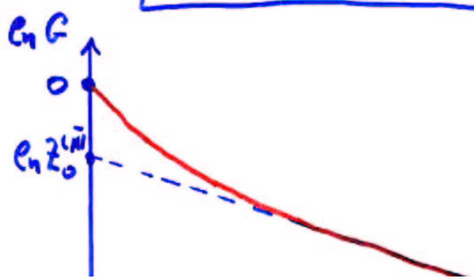

Moreover, it is possible to generate the N-phonon Green functions in the sector of given momentum **k**.

$$G_N(\mathbf{k},\tau,\mathbf{q}_1,\dots,\mathbf{q}_N) =$$

$$\langle vac \mid b_{q_N}(0)\dots b_{q_1}(0) a_p(0) a_p^\dagger(\tau) b_{q_1}^\dagger(\tau)\dots b_{q_N}^\dagger(\tau) \mid vac\rangle$$

Where

$$\mathbf{p}=\mathbf{k}-\sum_{i=1}^{N}\mathbf{q}_i$$

This gives both energy and phonon distribution of the quasiparticle

$$G_N(\mathbf{k},\tau \gg \Omega,\mathbf{q}_1,\dots,\mathbf{q}_N) = |\phi_N(\mathbf{k},\mathbf{q}_1,\dots,\mathbf{q}_N)|^2 e^{-E_{pol}(k)\tau}$$

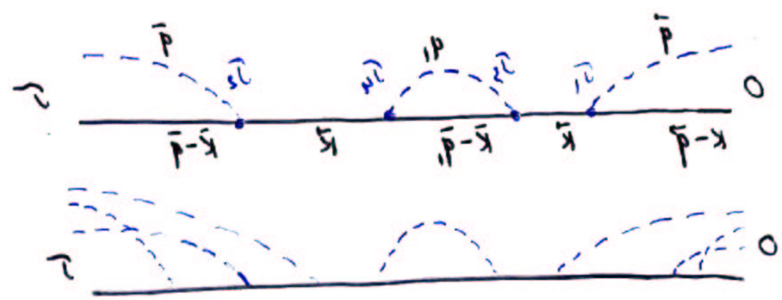

$$\sum_{q_1\dots q_N} G_N(\vec{k},\tau >> \Omega, \vec{q}_1,\dots,\vec{q}_N) = Z^{(N)} e^{-E_{pol}\tau}$$

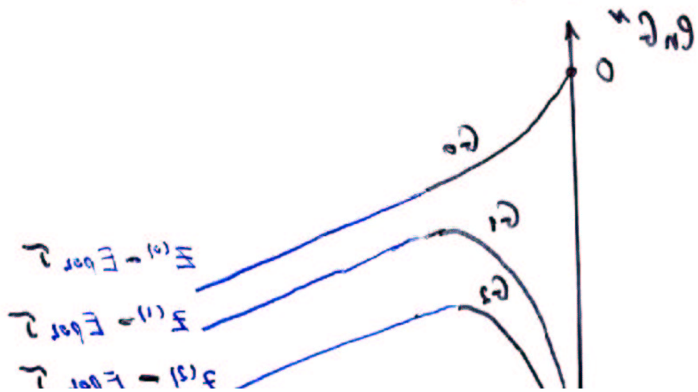

Spectral density $g(\omega)$.

$$g_{\mathbf{k}}(\omega) = \sum_\nu \delta(\omega - E_\nu(\mathbf{k}))\, |\langle \nu | a^\dagger_{\mathbf{k}} | \mathrm{vac}\rangle|^2$$

$$G(\tau) = \int_0^\infty g(\omega) e^{-\omega\tau} d\omega$$

This equation is "ill-defined" problem and solution is difficult due to "saw-tooth" instability.

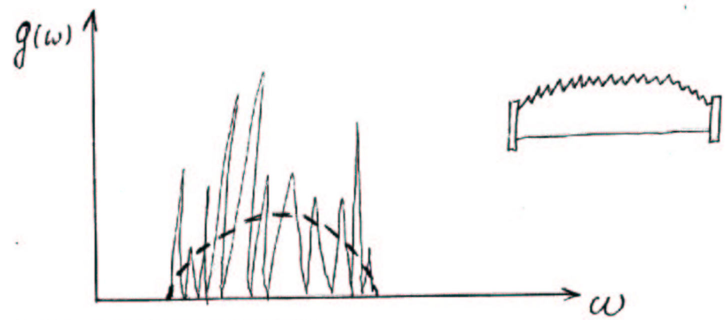

1. Regularization method.

$$+ \int_0^\infty F(g(\omega), g'(\omega), g''(\omega))$$

2. Maximal Entropy method.

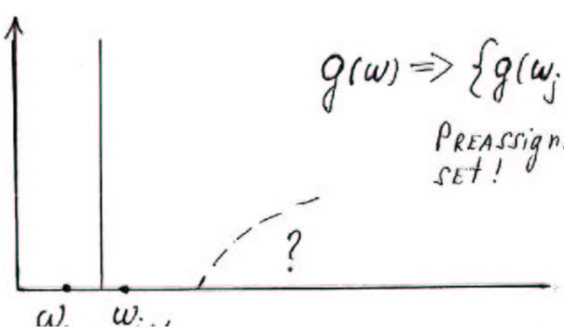

$g(\omega) \Rightarrow \{g(\omega_j);\ j = 1, 2, \ldots, N\}$

Preassigned discrete set!

We parametrise the spectral function $\tilde{\rho}(\omega)$ by a set of rectangulars:

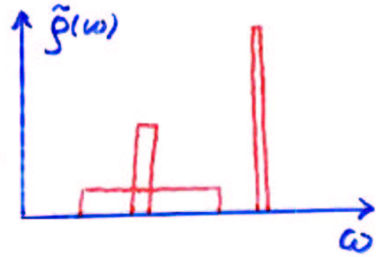

$$\boxed{\mathbb{C} = \{\{h_t, w_t, c_t\};\ t = 1, \ldots, K \quad \sum_t h_t w_t = 1}$$

① h_t, w_t, c_t are continuous variables

② K is not fixed

We start from randomly chosen initial configuration $\mathbb{C}$ and perform stochastically random minimization of the measure

$$\boxed{\delta_{\mathbb{C}} = \int_0^{\tau_{MAX}} \frac{|G(\tau) - \tilde{G}(\tau)|}{G(\tau)} d\tau \qquad \tilde{G}(\tau) = \int_0^\infty \tilde{\rho}(\omega) e^{-\omega\tau} d\omega}$$

① K is not fixed during minimization procedure

② All initial configurations $\mathbb{C}$ are are statistically independent.

③ Each final optimal configuration

After large amount L of stochastically independent runs we achieve self-averaging of saw-tooth noise

$$\boxed{\tilde{\rho}_{final}(\omega) = \frac{1}{L}\sum_{i=1}^{L}\tilde{\rho}_i(\omega)}$$

No approximation! No regularization! Exact in statistical limit due to linearity of the problem.

Note (!): this method is well defined for T=0 or very small T! In this case G(τ) can be calculated up to very large τ.

For large T the problem is inavoidable ill-defined.

Test of the spectral analysis.
Results, which follow, can not be obtained by any other known method.

E CARLO STUDY OF . . . 6335

PRB 62 DIAGRAMMATIC QUANTU

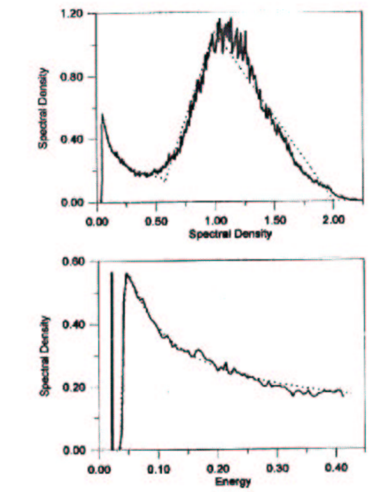

FIG. 16. Model spectral density (dashed line) and the result of spectral analysis (solid line). The position of the delta function is shown only in the lower panel.

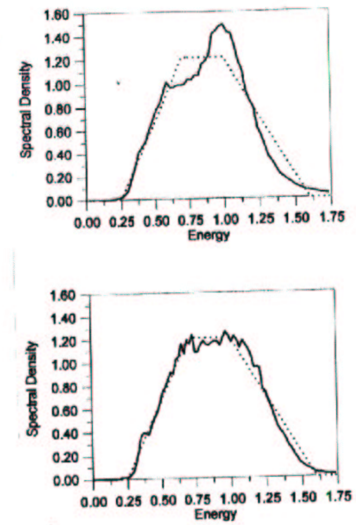

FIG. 17. The model spectrum (dashed lines) and results of spectral analysis (solid lines) for $\eta = 10^{-2}$ (upper panel) and $\eta = 10^{-3}$ (lower panel).

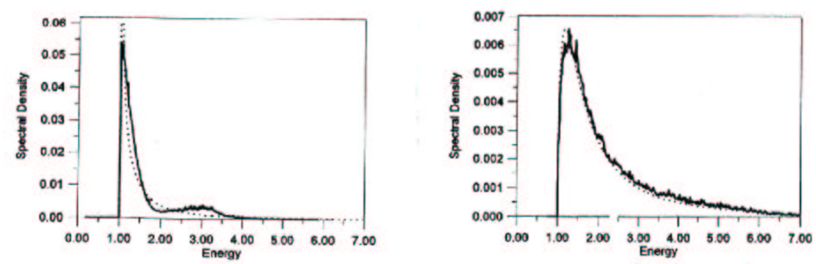

FIG. 13. The comparison of the numeric results (solid lines) and the perturbation-theory curves (dashed lines) for the spectral density of Fröhlich model with $\alpha = 0.05$ (upper panel) and the short-range interaction model with $\alpha = 0.05$ and $\kappa = 1$ (lower panel).

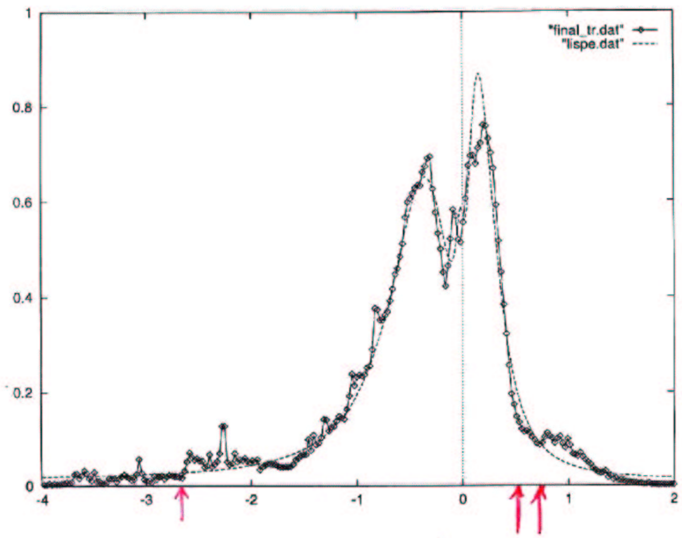

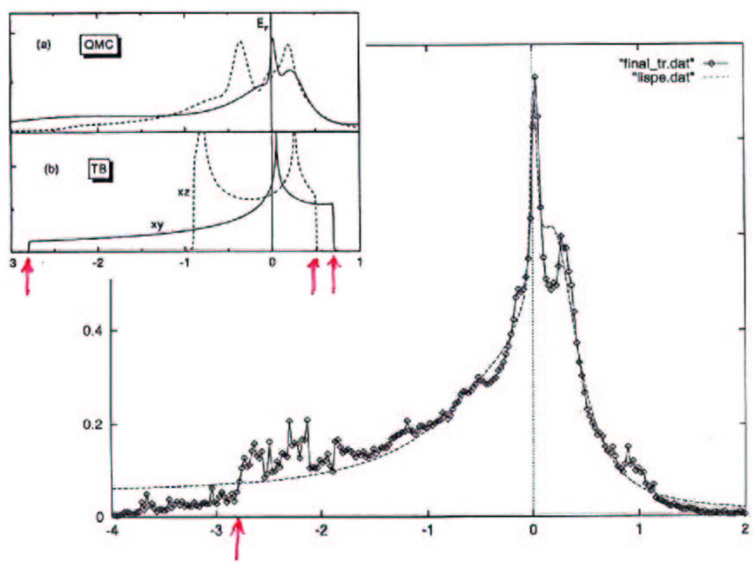

Fröhlich polaron.

MONTE CARLO STUDY OF . . . 6323

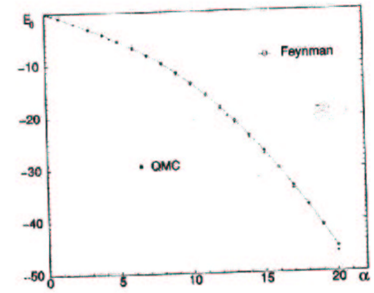

FIG. 4. Bottom of the polaron band E_0 as a function of α. The error bars are much smaller than the point size.

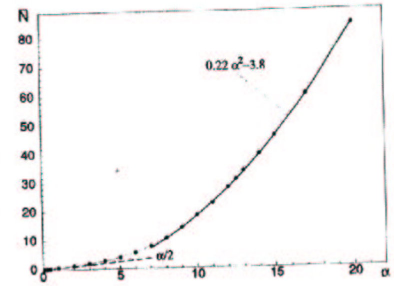

FIG. 8. The average number of phonons in the polaron ground state as a function of α. Filled circles are the MC data (calculated to the relative accuracy better than 10^{-3}), the dashed line is the perturbation theory result (4.1), and the solid line is the parabolic fit for the strong coupling limit.

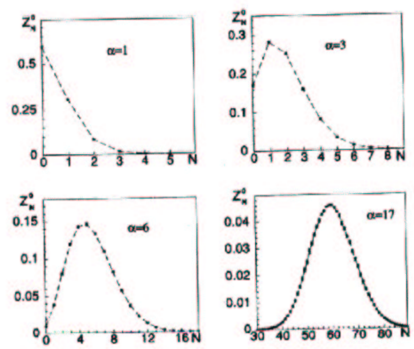

FIG. 7. Partial contributions of N-phonon states to the polaron ground state for various values of α. Error bars are shown, but are typically smaller than the point size. (The dashed lines are to guide the eye.)

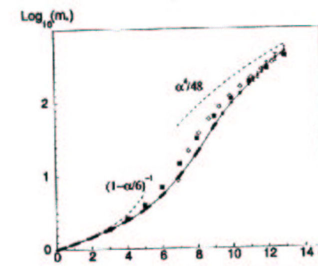

FIG. 5. Effective mass as a function of coupling parameter. Our MC data (circles interpolated by solid line; error bars are shown, but for $\alpha<9$ they are smaller than the point size, and as small as $10^{-3}m_*$ for $\alpha<6$) are compared with perturbation theory and strong-coupling-limit results (dashed lines), Feynman's approach (squares), and Feranchuk *et al.* variational approach (diamonds).

SELF-TRAPPING

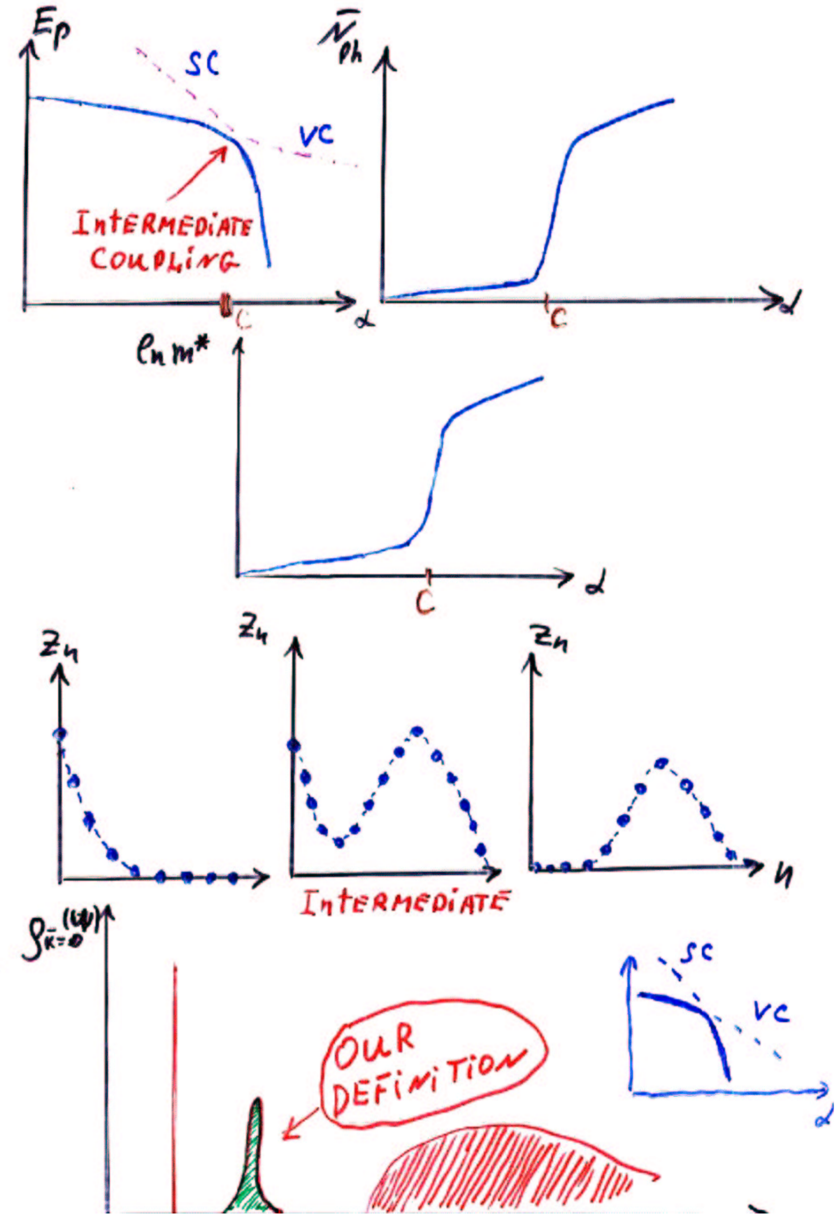

Rashba - Pekar
Exciton - Polaron

A. S. MISHCHENKO *et al.*

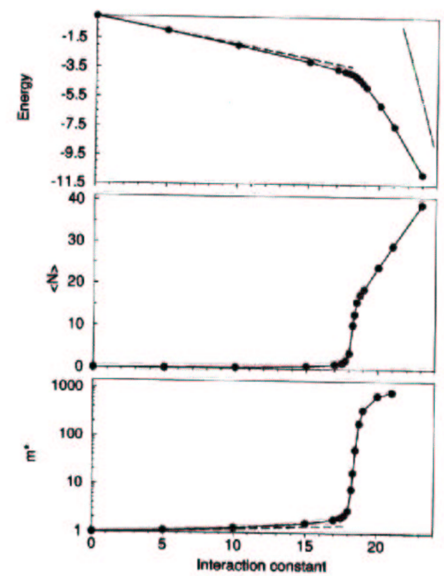

$$H_e=\sum_{\mathbf{k}} \varepsilon(\mathbf{k}) a_{\mathbf{k}}^{\dagger} a_{\mathbf{k}},$$

the Hamiltonian of the phonon bath

$$H_{\mathrm{ph}}=\sum_{\mathbf{q}} \omega_q b_{\mathbf{q}}^{\dagger} b_{\mathbf{q}}=\omega_0 \sum_{\mathbf{q}} b_{\mathbf{q}}^{\dagger} b_{\mathbf{q}},$$

and the standard density-displacement interaction[8]

$$H_{e-\mathrm{ph}}=\sum_{\mathbf{k},\mathbf{q}} V(\mathbf{q})(b_{\mathbf{q}}^{\dagger}-b_{-\mathbf{q}}) a_{\mathbf{k}-\mathbf{q}}^{\dagger} a_{\mathbf{k}}.$$

$$V(\mathbf{q})=\gamma(\mathbf{q})\left\{\frac{1}{[1+(\xi_e a_B q)^2]^2}-\frac{1}{[1+(\xi_h a_B q)^2]^2}\right\},$$

$$\gamma(\mathbf{q})=i(2\sqrt{2}\alpha\pi)^{1/2} q^{-1}.$$

SELF-TRAPPING OF POLARONS IN THE RASHBA- . . .

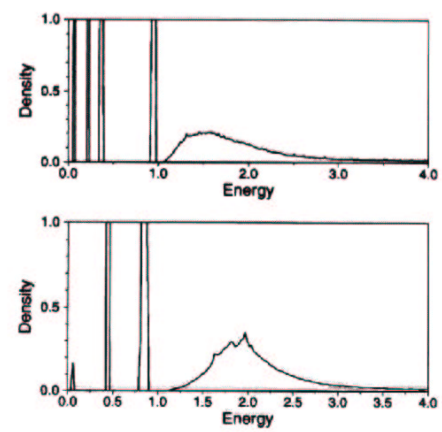

FIG. 3. The Lehman spectral function $S^{(\mathbf{k}=0)}$ at coupling constants $\alpha=18.35$ (upper panel) and $\alpha=18.75$ (lower panel).

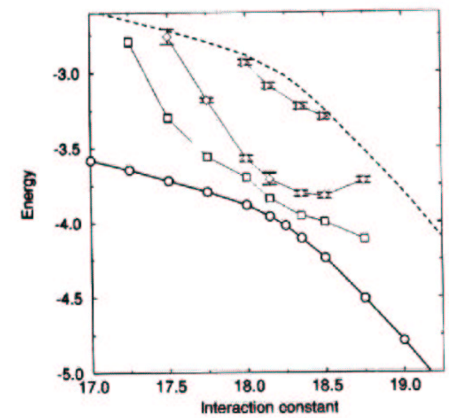

FIG. 4. Energies of the ground (circles) and excited stable (squares, diamonds, and triangles) states vs interaction constant. The dashed line is the threshold of incoherent continuum. Typical error bars for the first, second, and third excited states are 10^{-2}, 3×10^{-2}, and 4×10^{-2}, respectively.

PRL, vol. 87, p. 186402 (2001) E. Burovski.

Diagrammatic expansion for Coulomb ladder.

$$H_0 = \sum_{\mathbf{k}} \varepsilon_c(\mathbf{k}) e^\dagger_{\mathbf{k}} e_{\mathbf{k}} + \sum_{\mathbf{k}} \varepsilon_v(\mathbf{k}) h_{\mathbf{k}} h^\dagger_{\mathbf{k}}, \quad (1)$$

$$H_{\text{e-h}} = -N^{-1} \sum_{\mathbf{pkk'}} \mathcal{U}(\mathbf{p},\mathbf{k},\mathbf{k'}) e^\dagger_{\mathbf{p+k}} h^\dagger_{\mathbf{p-k}} h_{\mathbf{p-k'}} e_{\mathbf{p+k'}}. \quad (2)$$

Here $e_{\mathbf{k}}$ ($h_{\mathbf{k}}$) is the electron (hole) annihilation operator, $\varepsilon_c(\mathbf{k})$ ($\varepsilon_v(\mathbf{k})$) is the conduction (valence) band dispersion law, N is the number of lattice sites, and $\mathcal{U}(\mathbf{p},\mathbf{k},\mathbf{k'})$ is an attractive interaction potential.

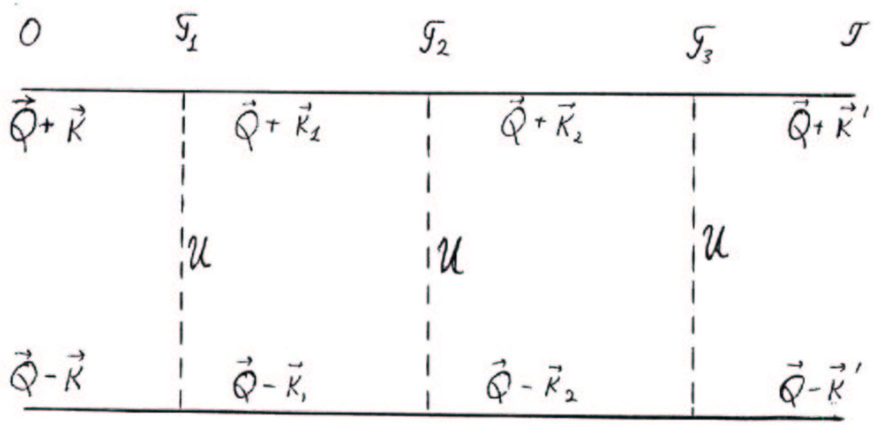

$$\boxed{G_{\vec Q}^{\vec K \vec K'}(\tau) = \langle 0 | e_{\vec Q+\vec K}\, h_{\vec Q-\vec K}\, h^\dagger_{\vec Q-\vec K'}(\tau)\, e^\dagger_{\vec Q+\vec K'}(\tau) | 0 \rangle}$$

Intermediate radius exciton.

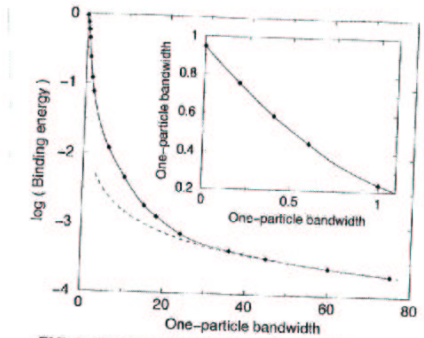

FIG. 2. The dependence of the exciton binding energy on the bandwidth $E_e = E_v$. Statistical errors are less than $5 \cdot 10^{-3}$ in relative units. The dashed line corresponds to the Wannier model. The solid line is the cubic spline, the derivatives at the right and left ends being fixed by the Wannier limit and perturbation theory, respectively. Insert: the initial part of the plot.

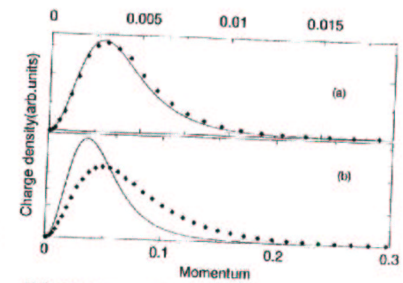

FIG. 3. The momentum dependence of the charge density $|\xi_{\mathbf{pk}}(g.s.)|^2 k^2$ for $E_c = E_v = 60$ (a) and $E_c - E_v = 10$ (b). Solid lines are the Wannier model result. Statistical errors are typically of order 10^{-4}.

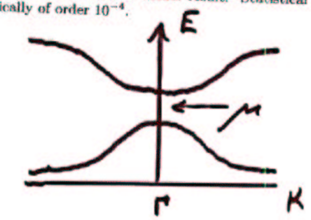

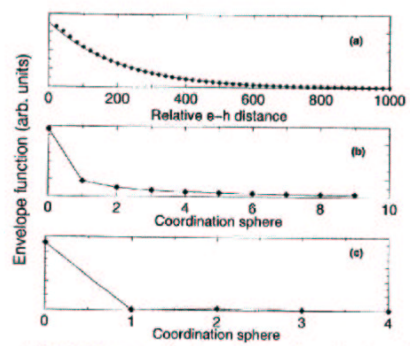

FIG. 4. The wave function of internal motion in real space: (a) Wannier [$E_c = E_v = 60$]; (b) intermediate [$E_c = E_v = 10$]; (c) near-Frenkel [$E_c = E_v = 0.4$] regimes [21]. The solid line in the panel (a) is the Wannier model result while solid lines in other panels are to guide an eye only. Statistical errorbars are of order 10^{-4}.

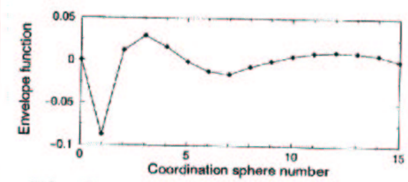

FIG. 5. The wave function of internal motion in real space for the optically forbidden monopolar ($W(2\mathbf{p}) = 0$) exciton defined by the following model parameters: $\tilde{E}_c = 1.5$, $\tilde{E}_v = 0$, $E_c = -0.5$, $E_v = 0.05$, $\epsilon = 10$, $V_0 = 0.578$. Statistical errorbars are of order 10^{-4}.

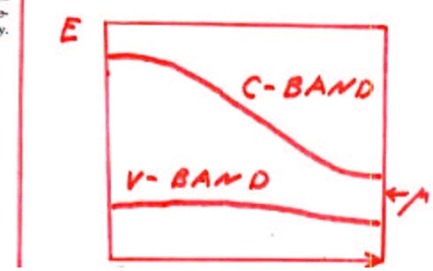

Diagrammatic expansion for charge transfer exciton: two-level system.

Quasiparticle dispersion for two bands $i = 1, 2$:

$$H_e = \sum_{i=1}^{2} \sum_{\mathbf{k}} \varepsilon_i(\mathbf{k})\, a^\dagger_{i,\mathbf{k}} a_{i,\mathbf{k}} .$$

Boson dispersion:

$$H_{ph} = \sum_{\mathbf{q}} \omega_{\mathbf{q}}\, b^\dagger_{\mathbf{q}} b_{\mathbf{q}} .$$

Quasiparticle-boson interaction:

$$H_{e\text{-}ph} = \sum_{i=1}^{2} \sum_{j=1}^{2} \sum_{\mathbf{k},\mathbf{q}} V_{ij}(\mathbf{q}) \left(b^\dagger_{\mathbf{q}} - b_{-\mathbf{q}} \right) a^\dagger_{i,\mathbf{k}-\mathbf{q}} a_{j\mathbf{k}} + h.c. \, .$$

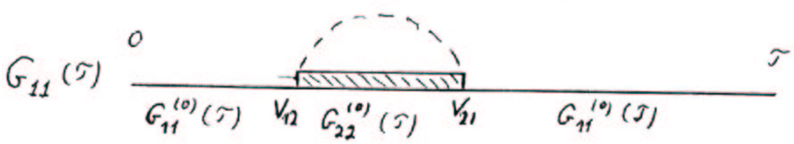

16 TOPOLOGICAL CLASSES.

A. S. Mishchenko and N. Nagaosa
Phys. Rev. Lett, v. 86, p. 4624(2001)

Charge transfer two-level exciton-polaron.

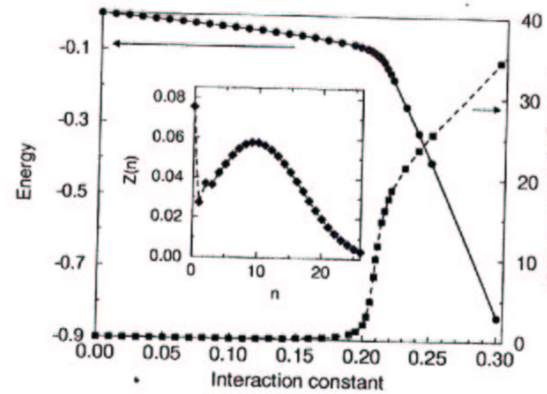

FIG. 1. Energy (solid line, circles) and $\bar{N}$ (dashed line, squares) dependence on γ_{12} at $\gamma_{11} = 0$ and $\gamma_{11} = 0.05$. Inset: Z-factors distribution for $\gamma_{12} = 0.2087$. The statistic error bars are much smaller than the point size.

Self-Trapping is possible in 1D in spite of Rashba-Toyozawa theorem!

PHYSICAL REVIEW B, VOLUME 64, 033101

Single-hole spectral function and spin-charge separation in the t-J model

A. S. Mishchenko,[1,2] N. V. Prokof'ev,[3] and B. V. Svistunov[2,3]

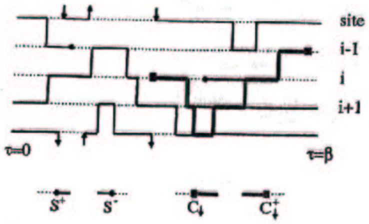

FIG. 1. World-line configuration describing quantum AFM with the hole; solid (dotted) lines correspond to spin-up (-down) states and the bold line describes the hole. Arrows indicate how periodic boundary conditions are used.

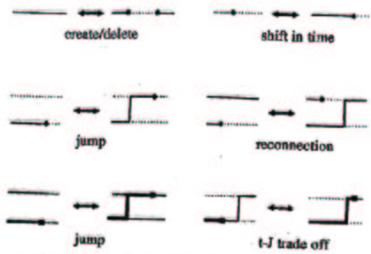

FIG. 2. Elementary Monte Carlo updates that form an ergodic set. We show updates for s^+ and $c_\uparrow^\dagger$ end points only since procedures for s^- and $c_\downarrow^\dagger$, $c_\uparrow$ are identical up to a change of notations (i.e., using proper incoming and outgoing lines).

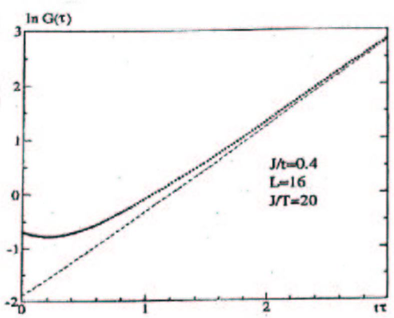

FIG. 4. $G_{k_0}(\tau)$ (circles) and the asymptotic line $Z_{k_0}e^{-E_{k_0}\tau}$ (dashed) for J/t=0.4 with Z_{k_0} and E_{k_0} obtained from the weight and position of the peak in the spectral function.

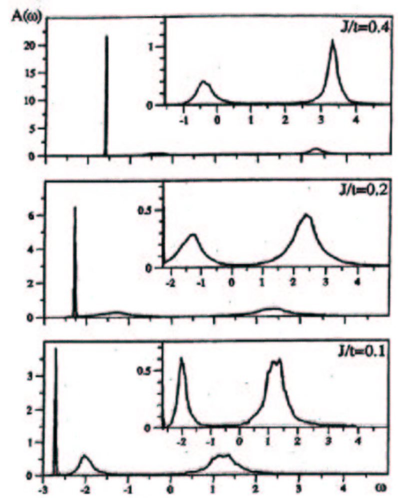

FIG. 5. Spectral functions for $J/t=0.4$, 0.2, and 0.1. Frequency is measured in units of t and the integral $\int d\omega A(\omega)$ is normalized to unity. These spectra were obtained for the 16×16 lattice at $T=J/20$.

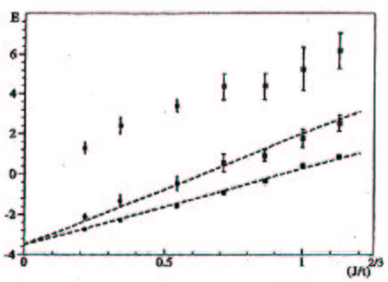

FIG. 6. Peak positions as functions of $(J/t)^{2/3}$. Data points for $J>0.4$ (squares) were taken from Ref. 15 [for $J=0.4\ t$, the second peak was not resolved in Ref. 15 because of large error bars in $G(\tau)$]. The two lines are fits $y(x)=a+b(J/t)^{2/3}$ with $a=-3.5\ t$, $b=3.77\ t$ for the ground state, and $b=5.5\ t$ for the first peak in continuum.

Lehman Function

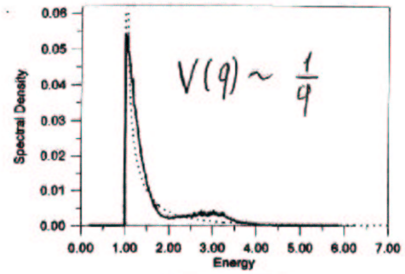

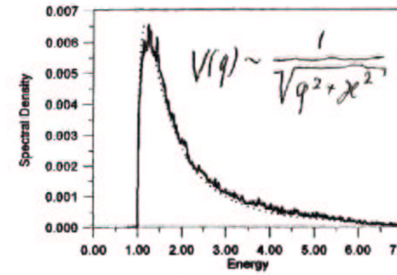

$$g_0(\omega) = \sum_\nu \delta[\omega - E_\nu(0)]\,|\langle\nu|a_0^\dagger|VAC\rangle|^2$$

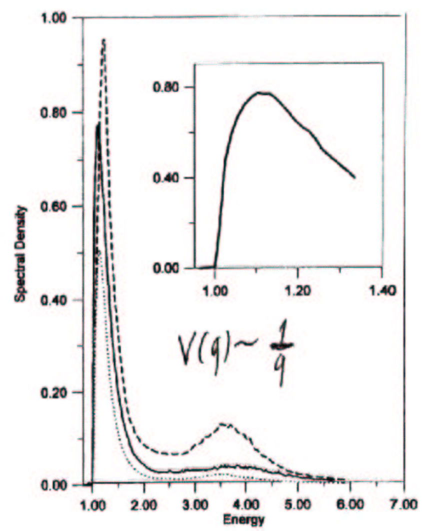

FIG. 14. The spectral density of Fröhlich polaron for $\alpha=0.5$ (dotted line), $\alpha=1$ (solid line), and $\alpha=2$ (dashed line), with energy counted from the position of the polaron. The initial fragment of the spectral density for $\alpha=1$ is shown in the inset.

6328 MISHCHENKO, PROKOF'EV, S

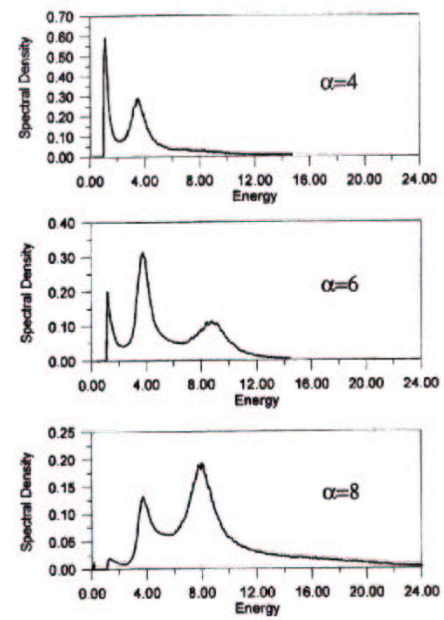

FIG. 15. Evolution of spectral density with α in the crossover region from intermediate to strong couplings. (The polaron ground-state peak is shown only for $\alpha=8$. Note, that the spectral analysis still resolves it, despite its very small weight $<10^{-3}$.) The energy is counted from the position of the polaron.

Relation to the real part of optical conductivity.

$m = \hbar = e = 1 \; ; \quad T = 0.$

$$\boxed{\langle \hat{\vec{P}}(\tau)\, \vec{P}(0) \rangle = \int_0^\infty e^{-\omega\tau}\, \bar{Q}^{(+)}(\omega)\, d\omega}$$

$$\boxed{\sigma(\omega) = \frac{\pi}{\omega}\, \bar{Q}^{(+)}(\omega)}$$

Sum Rule (DEVREESE)

$$\frac{1}{m^*} = \frac{1}{m} - 2 \int_0^\infty \frac{\bar{Q}^{(+)}(\omega)}{\omega}\, d\omega$$

$$\langle \hat{P}(\tau)\, P(0) \rangle =$$

$$= \frac{1}{2}\frac{1}{\beta}\int_0^\beta dt \sum_{n=0,2,\ldots}^{\infty} \int_0^\beta d\tau_n \int_0^{\tau_n} d\tau_{n-1} \ldots \int_0^{\tau_2} d\tau_1\; \vec{K}(t+\tau)\, \vec{K}(t) \,*$$

$$\int d\vec{q}_2 \ldots \int d\vec{q}_n\; |V(\vec{q}_2)|^2 \ldots |V(\vec{q}_n)|^2 \,*$$

$$\sum_\nu \langle \nu |\, a^+_{\vec{K}-\vec{q}_2}(\tau_1)\, a_{\vec{K}}(\tau_1)\, [\, b^+_q(\tau_1) - b_{-q}(\tau_1)] \ldots \quad |\nu\rangle$$

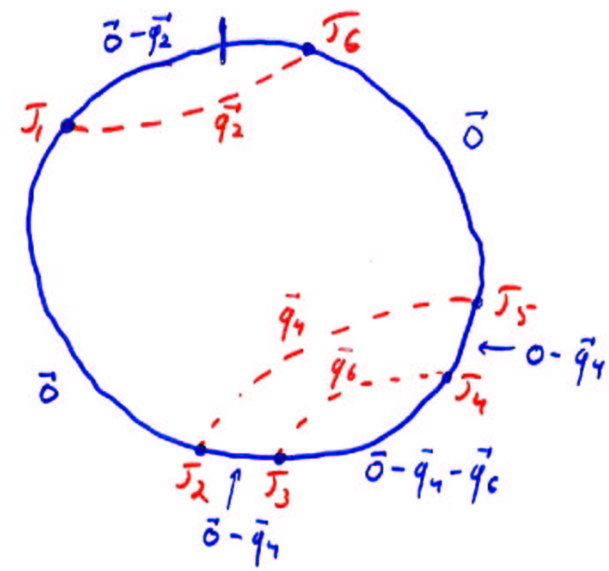

$$D = |V(\vec{q}_2)|^2 |V(\vec{q}_4)|^2 |V(\vec{q}_6)|^2\, \mathcal{D}(\vec{q}_2, \tau_1-\tau_6)\, \mathcal{D}(\vec{q}_4, \tau_5-\tau_2)$$

$$\mathcal{D}(\vec{q}_6, \tau_4-\tau_3)\; G^{(0)}(\vec{0}, \tau_6-\tau_5)\; G^{(0)}(-\vec{q}_2, \tau_1-\tau_6)$$

$$G^{(0)}(\vec{0}, \tau_2-\tau_1)\; G^{(0)}(-\vec{q}_4, \tau_3-\tau_2)\; G^{(0)}(-\vec{q}_4-\vec{q}_6, \tau_4-\tau_3)$$

$$G^{(0)}(-\vec{q}_4, \tau_5-\tau_4)$$

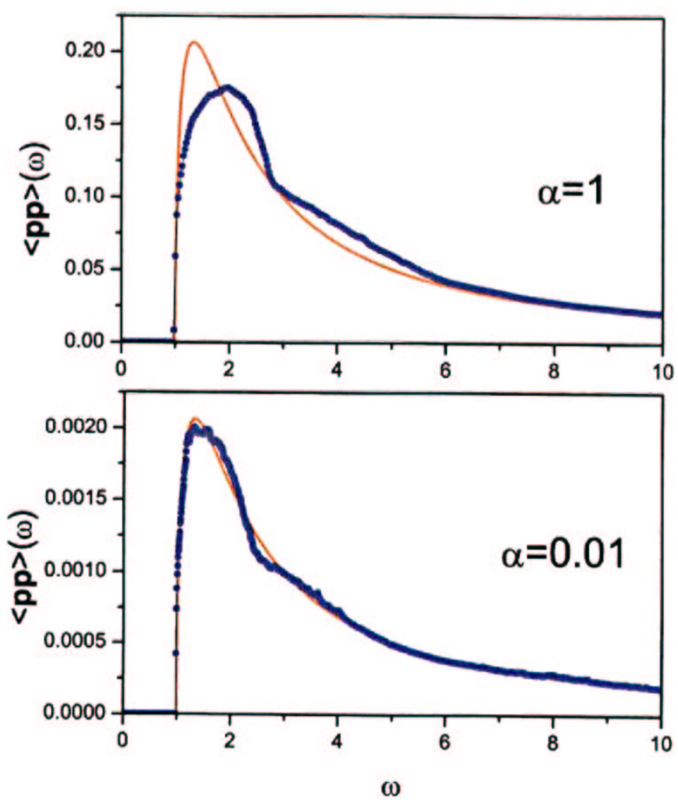

α=1
α=0.01
<pp>(ω)
ω

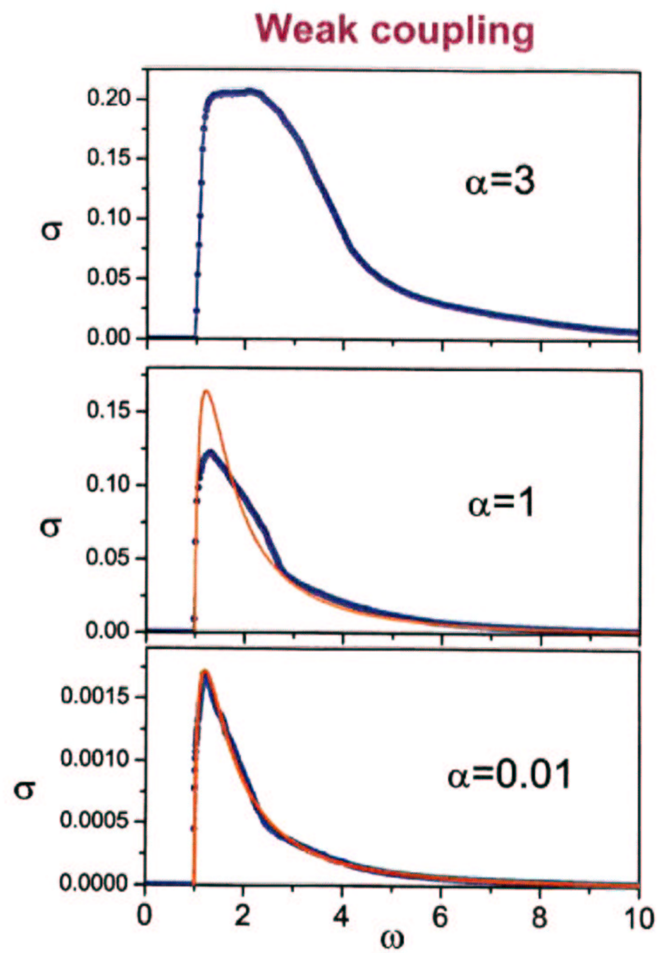

Weak coupling
α=3
α=1
α=0.01
σ
ω

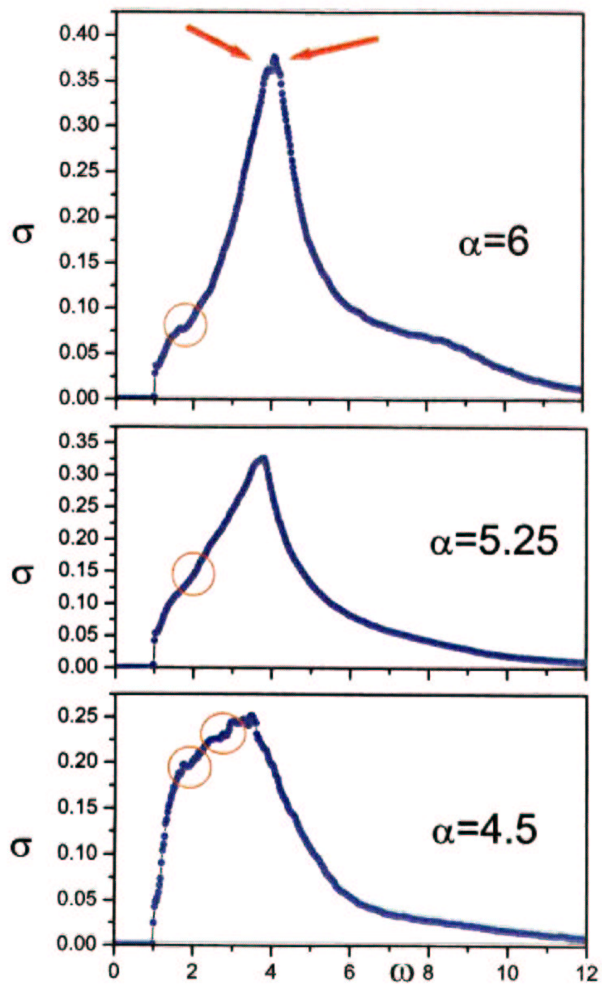
σ
α=6
α=5.25
α=4.5
ω

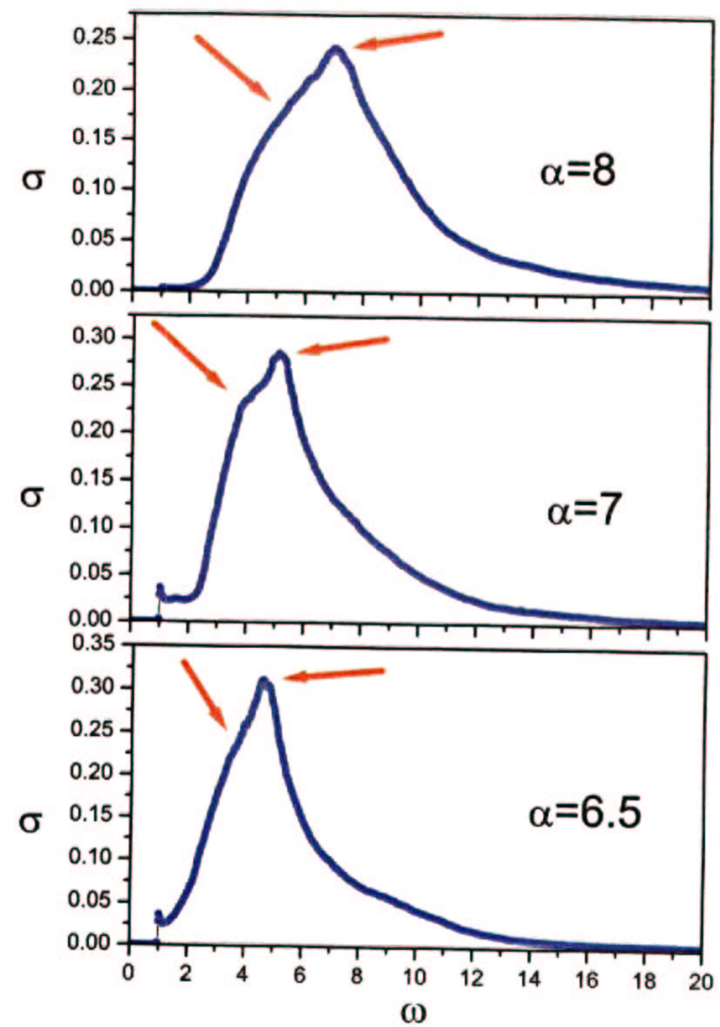
σ
α=8
α=7
α=6.5
ω

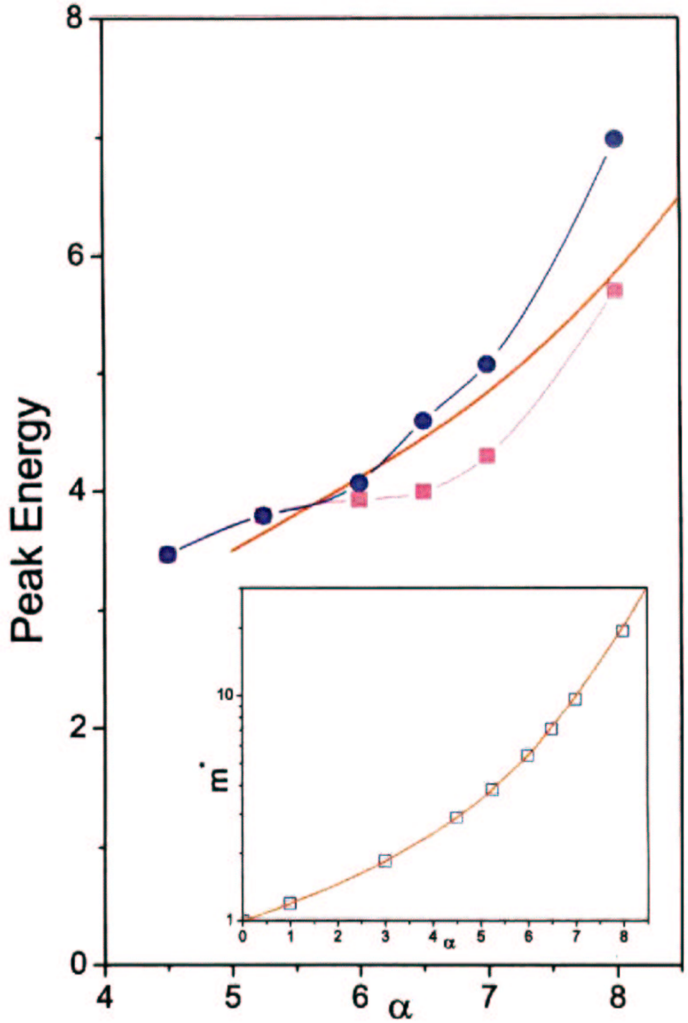

$$H_{t-J} = -t \sum_{i,j}^{nn} \sum_{\sigma} \left(c_{i\sigma}^{\dagger} c_{j\sigma} + h.c. \right) + J \sum_{i,j}^{nn} \mathbf{S}_i \mathbf{S}_i$$

$$H_{hole-ph} = \omega \sum_i b_i^{\dagger} b_i + \gamma \sum_i \sum_{\sigma} c_{i\sigma}^{\dagger} c_{i\sigma} \left(b_i^{\dagger} + b_i \right)$$

Spin-wave approximation

$$H_{t-J} = \sum_k \epsilon_k h_k^{\dagger} h_k + \sum_k \kappa_k \alpha_k^{\dagger} \alpha_k + \sum_{k,q} M_{k,q} \left[\alpha_q h_k^{\dagger} h_{k-q} + \alpha_q^{\dagger} h_{k-q}^{\dagger} h_k \right]$$

$$H_{hole-ph} = \omega \sum_i b_k^{\dagger} b_k + \gamma \sum_{k,q} h_k^{\dagger} h_{k-q} \left(b_q^{\dagger} + b_{-q} \right)$$

Where

$$\kappa_k = 2J\sqrt{1 - \lambda_k^2}$$

$$\lambda_k = (\cos k_x + \cos k_y)/2$$

$$M_{k,q} = 4t(u_q \lambda_{k-q} + v_q \lambda_k)$$

$$u_k = \sqrt{\frac{1+\nu_k}{2\nu_k}}; v_k = -sign(\lambda_k)\sqrt{\frac{1-\nu_k}{2\nu_k}}$$

$$\nu_k = \sqrt{1 - \lambda_k}$$

t-J model

—— Hole Green function

—— Magnon Green function

Non-crossing approximation for mag works well for $J/t \leq 0.3$

t-J-phonon model

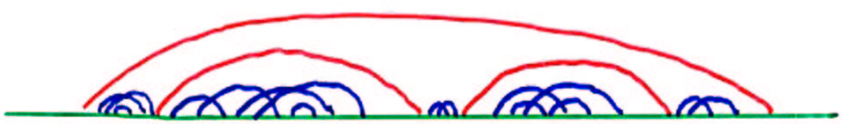

Phonon propagators —— can not cross magnon propagators but can cross each other

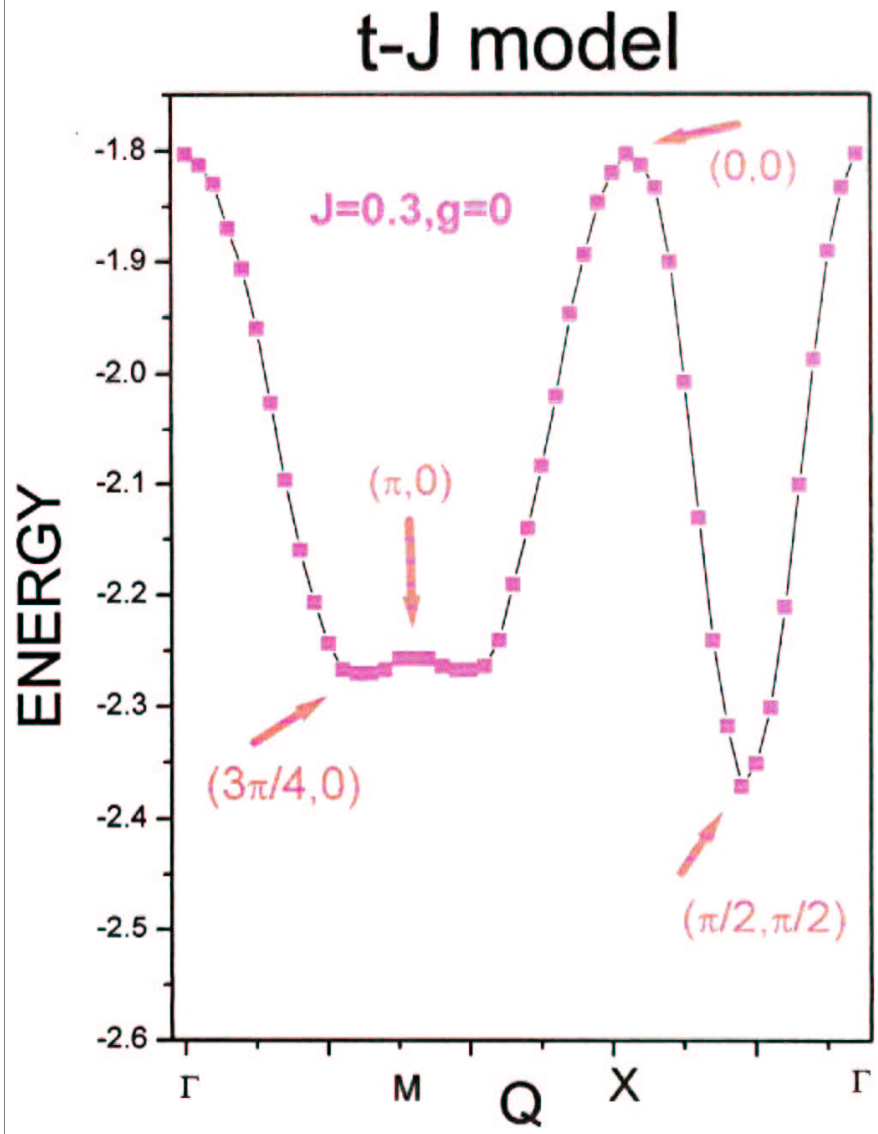

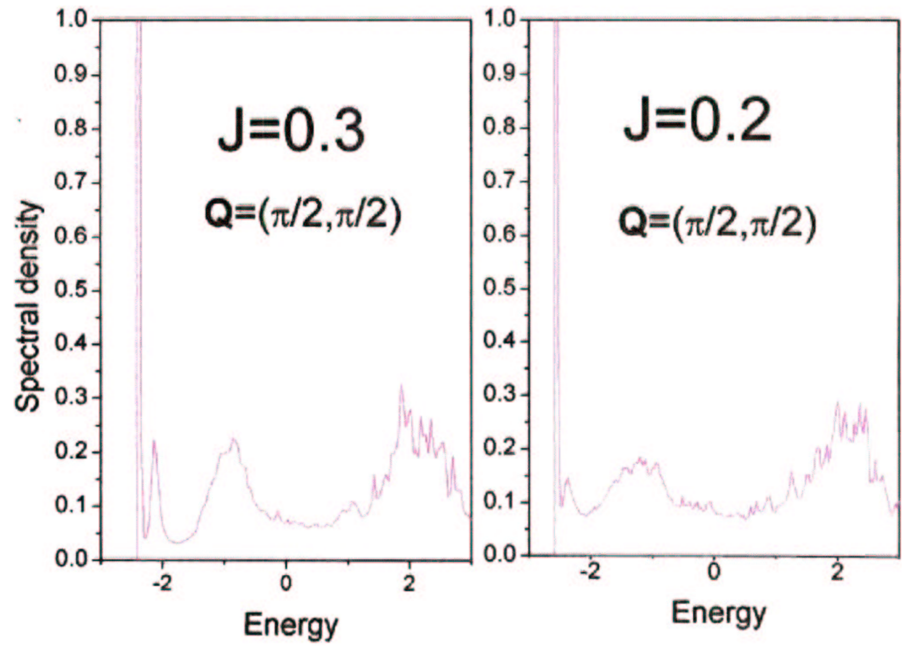

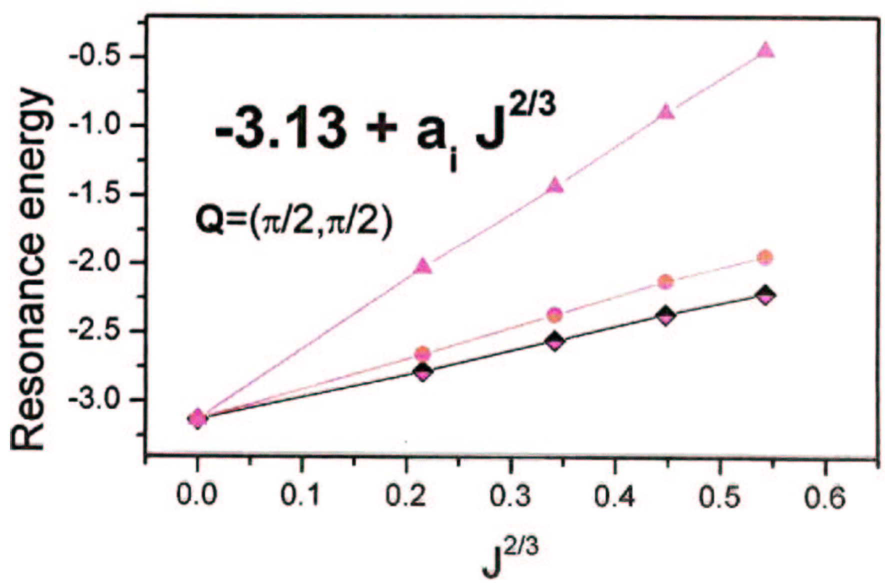

$t=1,\ \omega=0.1$

$g=\gamma^2/(8t\omega)$

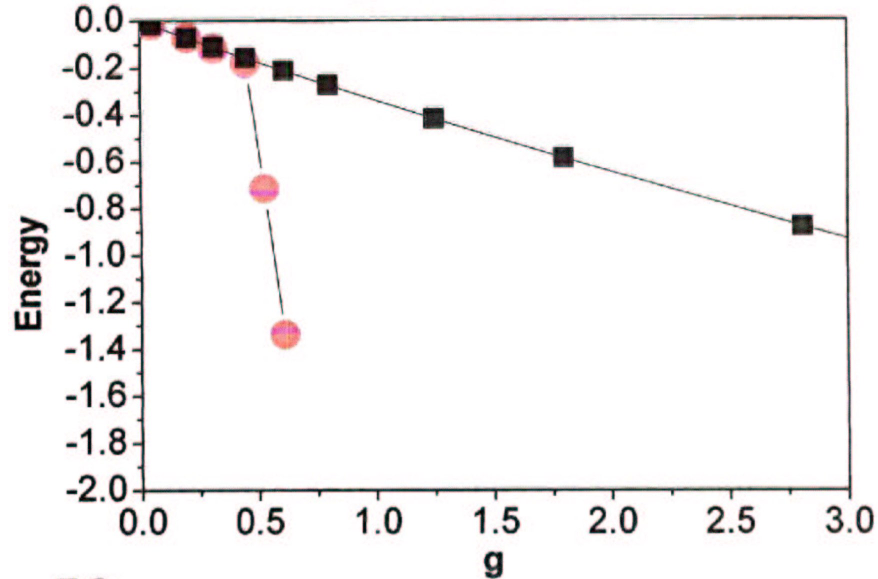

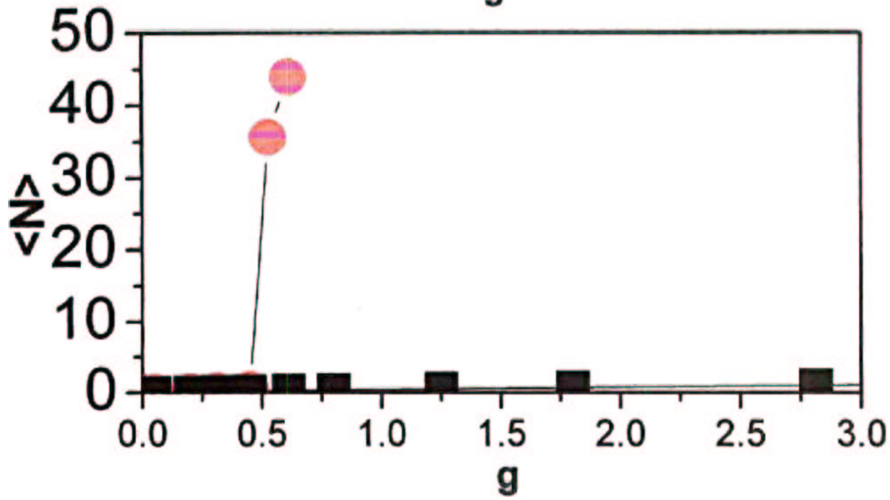

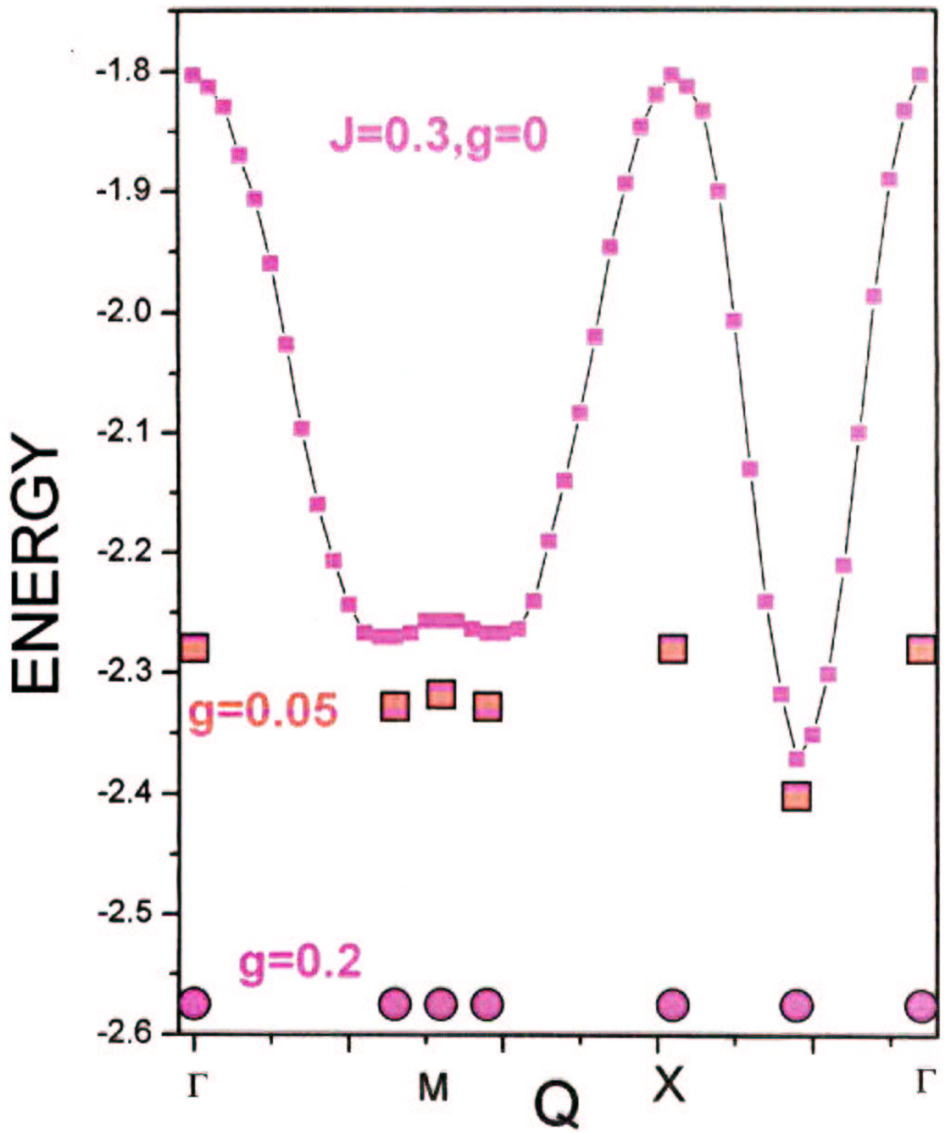
J=0.3,g=0
g=0.05
g=0.2
ENERGY
-1.8
-1.9
-2.0
-2.1
-2.2
-2.3
-2.4
-2.5
-2.6
Γ
M
Q
X
Γ

J=0.3, g=0.2

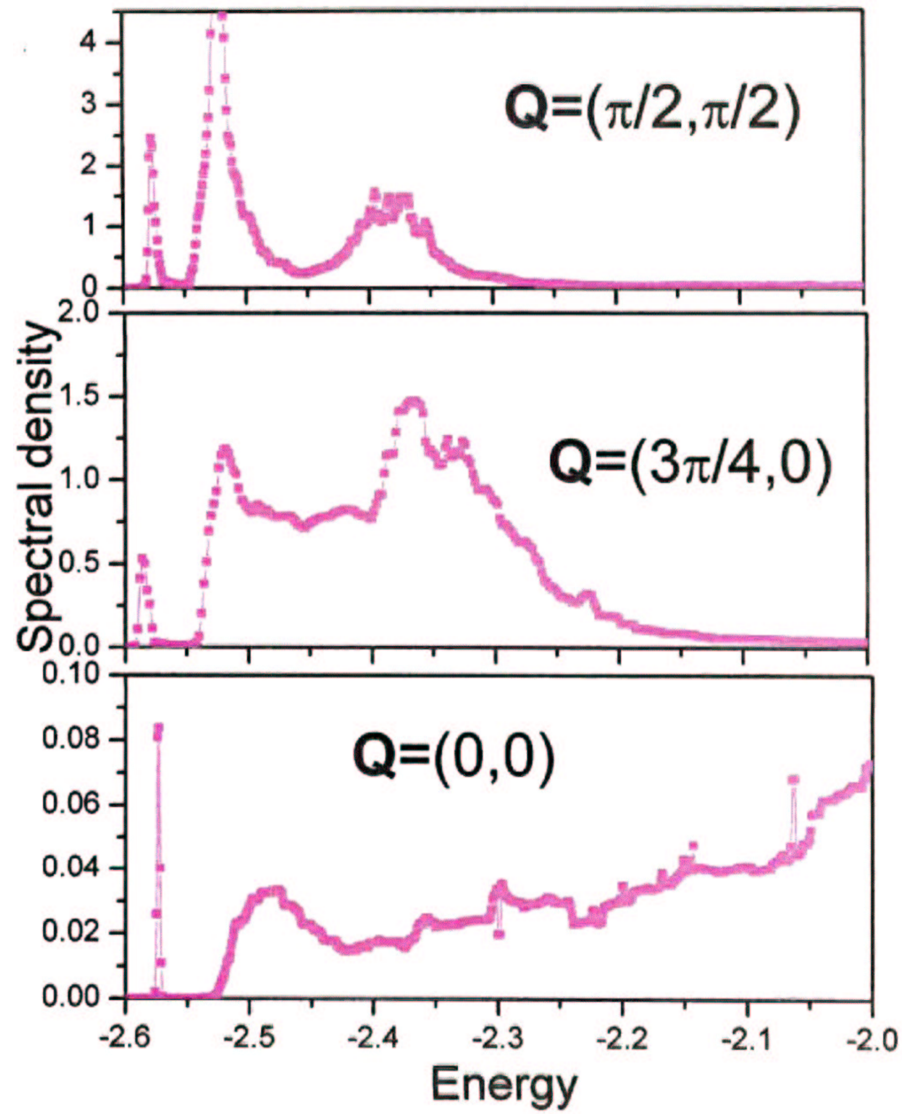
Q=(π/2,π/2)
Q=(3π/4,0)
Q=(0,0)
Spectral density
Energy
-2.6
-2.5
-2.4
-2.3
-2.2
-2.1
-2.0

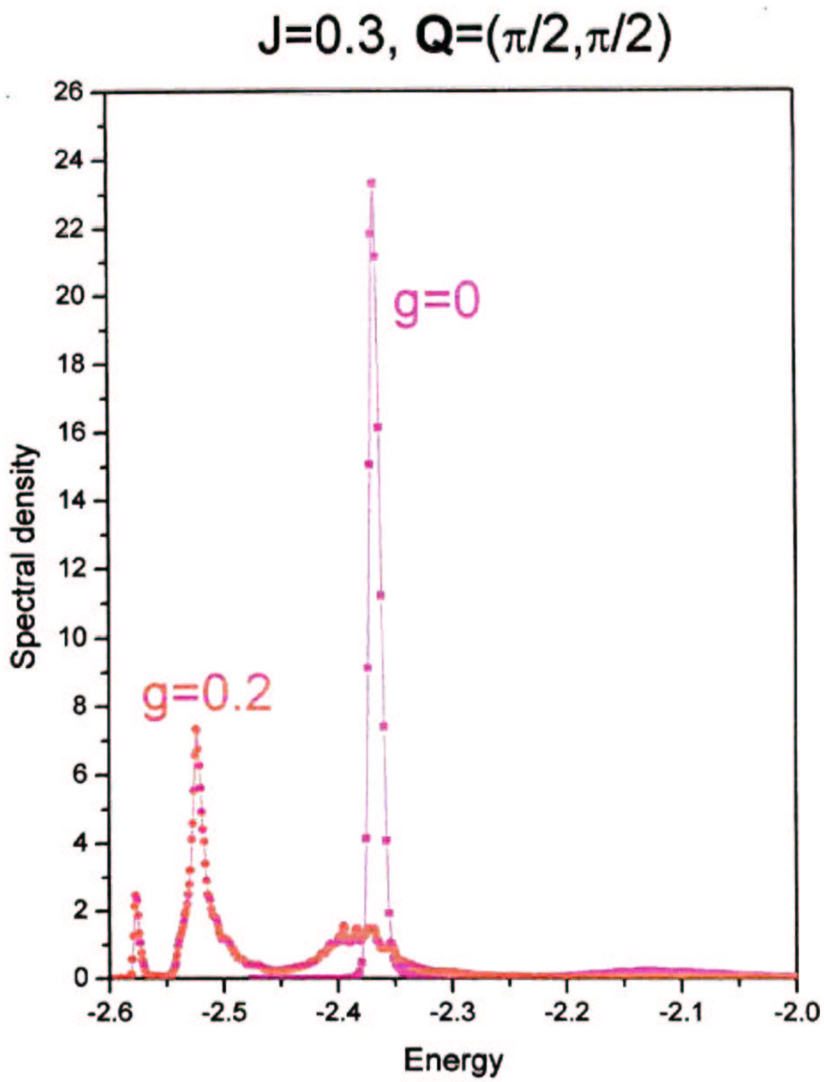

- The method of exact generation of Matsubara Green function and the method of exact analytic continuation to the real frequencies are powerful methods to study many-particle properties of the quasiparticles in bathes of bosonic excitations.
- Exciton can be treated exactly for any realistic model.
- Phenomenon of "self-trapping" was not understood well. New feature are found by our method.
- Magical number '4' exists for Fröhlich polaron model.
- Interaction of the hole with magnons enhances the role of hole-phonon interaction.